

## Approaches on vertical stability and shape control of KSTAR plasmas in the presence of intrinsic ferromagnetic material

Sang-hee Hahn 1), Y.K. Oh 1), Y.M. Jeon 1), S.W. Yoon 1), W. C. Kim 1), J.H. Choi 1), J. K. Jin 1), D. K. Lee 1), Y.S. Kim 1), H. L. Yang 1), J. G. Pak 1), K. I. You 1), J. A. Leuer 2), M. L. Walker 2), N.W. Eidiets 2), A.S. Welander 2), D. Mueller 3), S. A. Sabbagh 4) and D. A. Humphreys 2)

1) National Fusion Research Institute, Daejon, Republic of Korea

2) General Atomics, San Diego, CA, USA

3) Princeton Plasma Physics Laboratory, Princeton, NJ, USA

4) Columbia University, New York, NY, USA

E-mail contact of main author: hahn76@nfri.re.kr

**Abstract.** In KSTAR, the choice of Incoloy908 as a jacket material of the superconductors was expected to introduce large uncertainties to the measurement of the magnetic field profiles and hence the quality of plasma controls. However, from the experiments in the 2009 plasma campaign, the effect of additional ferrite fields was strongest at the burn-through phase, but gradually decreased as the PF coil currents saturated to its higher value. It has been also shown that feedback controls of plasma current ( $I_p$ ) and major radius ( $R_p$ ) are not sensitive to that additional magnetic field. In order to increase controllability, the magnet system and in-vessel structures of the KSTAR were recently upgraded for the 2010 fall campaign. At first, breaking four up/down symmetric connections of the 7 pairs of PF coil system guaranteed intrinsic vertical position controls. Second, by allowing higher PF coil current and upgrading grid power, the saturation of the incoloy908 is expected to occur earlier in the discharge and its influence becomes smaller consequently. Finally, the installations of Cu in-vessel vertical stabilization coils located behind newly introduced Cu passive stabilizers increases the stability margin for magnetic controls and allow development of diverted plasmas. The design of the up/down symmetric passive plates was analyzed by dynamic simulations based on a rigid response model to determine trade-off of the  $n=0$  passive stabilizing effects for the worst case. With these resources, the initial approach to create a diverted/double-null shaped plasma is described in this paper. An experimental approach of dealing with the error field at the X-point is suggested with incorporation with the standard RTEFIT/isoflux algorithms. The final plasma pulse scenario is expected to contain a feedforward breakdown scenario provided by offline calculations,  $I_p$  ramp up plus kappa feedback until  $I_p = 500$  kA and applications of isoflux with the X-point feedbacks. The approach is expected to be validated by separate simulations based on the 2009 data and to be illustrated with experimental results from the 2010 fall campaign.

### 1. Introduction

The importance of shape control of tokamak plasmas cannot be overemphasized for any modern tokamak research, especially in the high-beta regime which is one of the ultimate targets of KSTAR[1]. Because of the concept of magnetic confinement, any insertion of ferromagnetic materials in a tokamak had been regarded as a source of large uncertainties in the estimation of even basic parameters, such as plasma position or height of the X-point. However, recent research on the blanket modules for ITER suggests that we cannot avoid the choice of massive bulk metals that could have sufficient non-linear influence to affect the magnetically confined plasmas. In KSTAR, the choice of Incoloy908 as a jacket material of the Nb<sub>3</sub>Sn superconductors has introduced weak ferrites ( $\mu \sim 10$  at 4.5 Kelvin) into all 16 toroidal field (TF) coils and 5 pairs of the inner (blue) poloidal field (PF) coils as shown in Fig. 1. Since the coupled poloidal flux by these inner coils produces complex ferromagnetic fields, it became difficult to predict the exact magnetic field which each coil produces.

Fortunately, in the last plasma campaign, extensions of the plasma pulse to  $\sim 3$  seconds with robust bipolar PF current control produced significant data to quantify the influence of

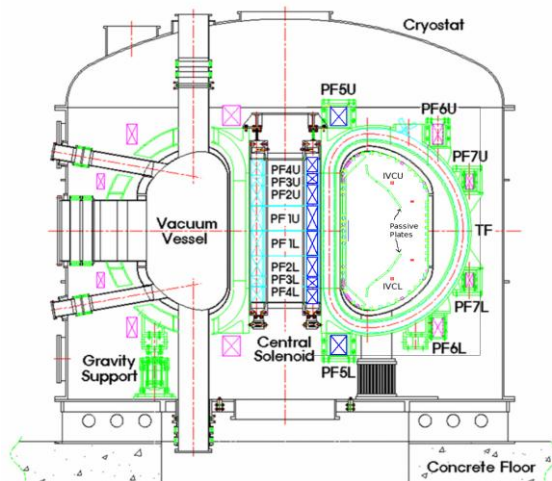


**Fig. 1. Coil & structure geometry of the KSTAR in 2010.**

## 2. Sensitivity study of the limited plasmas

Until the second plasma campaign of the KSTAR taken in 2009, the availability of the actuators were very restricted [4]: The maximum PF current level has been limited to  $\pm 4$  kA/turn, which can provide almost 1.3 Wb in principle, while the available poloidal flux for the startup was the same as in 2008 (less than 0.9 Wb) due to the blip resistor circuit insulation criteria ( $V_{\text{blip}} < 3\text{--}5$  kV). Hence the coil current levels of the inner PFs have been smaller than 4 kA/turn during the most time of the discharge. Since the up/down symmetry connections for the PF coils was maintained in last two years, controls for plasma vertical position ( $Z_p$ ) was impossible.

In this situation, there remained unsaturated ferrites [2] even in the initial magnetizations (IM) before the fast swing for plasma breakdown occurs, and at the moment of breakdown the influences of the incoloy fields were strongest to produce  $\sim 100$  G in maximum, which made the decay index unfavorable to the startups [5]. However, the new addition of the bipolar current controllability of all the PF coil power supplies gave us a new chance to increase the plasma current ( $I_p$ ) flattop with the coil current. Under the relatively higher coil currents in the  $I_p$  flattop afterwards, it has been also shown empirically that feedback controls of plasma

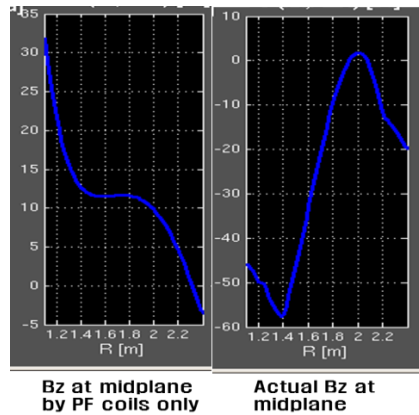


**Fig. 2. Vertical field (Bz) reconstructions produced by PF currents (left) and real measurement (right).**

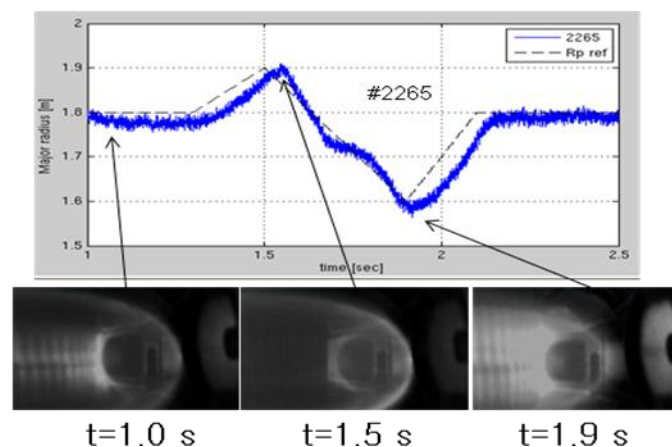


**Fig. 3. Plasma major radius (Rp) controls matching with the fast-frame CCD camera (380frames/sec) in the circular plasmas.**

Incoloy908. It was observed that remnant field effects from the incoloy908 in the TF coil jackets vanish when the TF coils are charged to produce more than 1 Tesla [2]. The ferromagnetic field produced by the excitation of a single coil approaches to a saturated [2, 3] value as the coil current on inboard PF coils increases to 4 kA/turn. In this paper we will review some experimental aspects on the influences of the materials in the limited plasma situations first, describe additional control elements introduced to the KSTAR, and conclude with the final approaches on the plasma shape controls with experimental data.

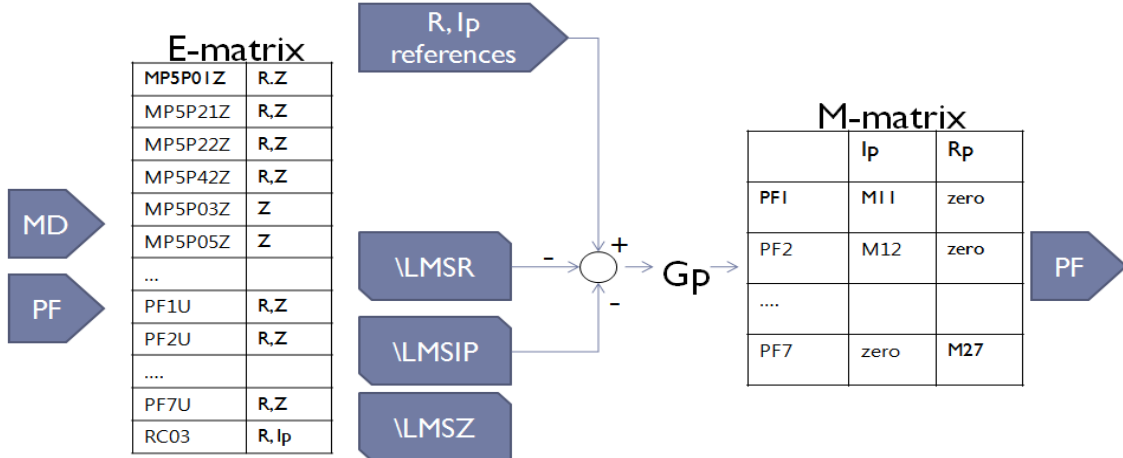


**Fig. 4. Design of the R, Z & Ip feedback loop of the KSTAR PCS: the Estimator matrix (E-matrix) consists of response weights on magnetic probes and PF coils, and multiplication matrix (M-matrix) determines how the PCS responses are distributed on each actuator.**

current ( $Ip$ ) and major radius ( $Rp$ ) are not very sensitive to the incoloy908 effect, as shown in Fig. 3. The measured major radius by magnetic probes and PF contributions matched to the one obtained from fast CCD camera images. It is very difficult to know how the incolloys affected the vertical position, because of the up/down asymmetric structures of the surrounding structures. In theory, the effects of the incolloys should be up/down symmetric if the current sources are symmetric. In the static conditions in last 2 years, the measurement matched to the up/down symmetric static model [2].

The discharge shape control design utilized algorithms adapted from DIII-D PCS for  $Rp$ ,  $Zp$  and  $Ip$ . The influence of the ferrites is mostly to the estimator matrix (E-matrix) shown in Fig. 4: the E-matrix consisted of magnetic probes with good conditions, and the additional magnetic field caught to the magnetic probes affected to the values of the  $Rp$  and  $Zp$ . Since the real-time  $Ip$  was measured by a set of Rogowski coils installed inside the vacuum vessel [6], and there were no ferrites installed inside the vessel, the  $Ip$  feedbacks were not affected by the material fields which were outside of the loop in the Ampere's law. It is very difficult to know how much each PF coil produces the additional field in time because of the strongly coupled field profile as well as hysteresis which depends on the time history. The static measurement with a single coil said that the inner PF structures produce 10~15% of the poloidal flux within 4 kA/turn, hence determining magnetic contributions from the PF coils was always erratic.

Hence a new approach has been made for the estimators based on the differences from various magnetic contributions measured by magnetic diagnostics inside the vessel to eliminate any background field contributions. A simplest estimator [2, 7] consisting of a pair of magnetic probes inside/outside midplane has been tested in the experiments. As shown in Fig. 5, the measurement and the coordinates obtained from analysis of the fast CCD TV fairly matched.

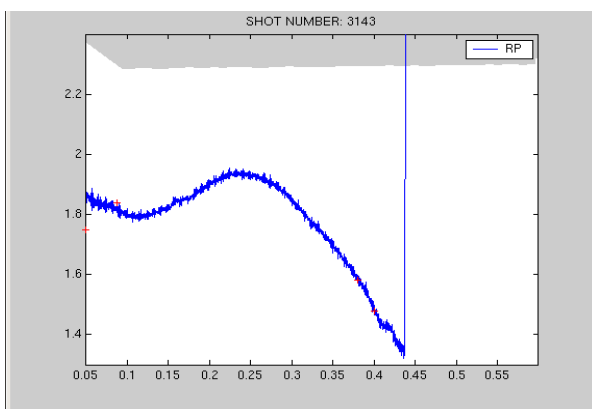


**Fig. 5. Comparison of the Rp estimators composed by 4 midplane probes (blue) and Rp estimate from the fast CCD TV (red +).**

### 3. Approach to the diverted plasmas

#### 3.1. Installations of additional shape control actuators

In order to increase controllability, we recently upgraded the PF coil system by breaking of the up/down symmetric connections of four of the seven PF coil pairs (PF3U/L to PF6U/L), and installed a pair of Cu in-vessel vertical stabilization coils (IVCU/L in Fig. 1) behind newly introduced Cu passive stabilizers[8]. A simpler version of the passive stabilizers was installed, which had four electrical cuts bridged with replaceable gap resistors on each upper/lower passive plate and removed all Cu current bridges in the original “saddle type” design[8]. In order to determine the optimal values of the gap resistors for vertical stabilizations, dynamic simulations based on the rigid response model were done [9]. According to the simulations, the natural vertical growth rate on worst cases ( $I_p \sim 2$  MA with very low beta) was  $\sim 100$  rad/sec, assuming the one-turn toroidal resistance of each upper/lower plate as 2.4 mOhms. Under this design the stability margin increases by a factor of 10 than the design with no passive plates. As shown in Fig. 6, the maximum coil current required for IVC is reduced by a factor of 3 compared with the original design, which was expected to reduce the influence of Incoloy908 by the IVC itself as well as decreasing the contributions of the stabilizer current, which is very difficult to measure due to the availability of the installation spots for any diagnostics.

The new set of in-vessel vertical stabilization coils (IVC) power supply (PS) has been installed and tested up to  $\sim 5$  kA/turn with 1.2 MA/s of rampup ability. The PCS provides coil current feedback with voltage commands into the IVC PS, which is a PWM switching power supply with 4 kHz of switching frequency. Two kinds of control interfaces utilizing analog/digital have been developed and tested. Each interface makes different system responses and, consequently, has different best gain set. Figure 7 shows the design of the faster coil current regulation loop with  $\sim 550$  us of time delays. A pair of optic isolators was installed to the interfaces between the PCS output and the IVC PS for avoiding any high-

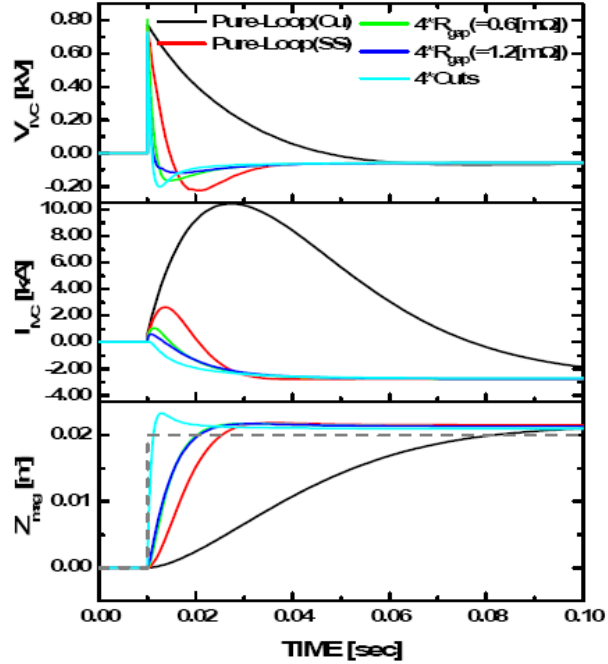


**Fig. 6. Comparison of the Rp estimators composed by 4 midplane probes (blue) and Rp estimate from the fast CCD TV (red +).**

this design the stability margin increases by a factor of 10 than the design with no passive plates. As shown in Fig. 6, the maximum coil current required for IVC is reduced by a factor of 3 compared with the original design, which was expected to reduce the influence of Incoloy908 by the IVC itself as well as decreasing the contributions of the stabilizer current, which is very difficult to measure due to the availability of the installation spots for any diagnostics.

The new set of in-vessel vertical stabilization coils (IVC) power supply (PS) has been installed and tested up to  $\sim 5$  kA/turn with 1.2 MA/s of rampup ability. The PCS provides coil current feedback with voltage commands into the IVC PS, which is a PWM switching power supply with 4 kHz of switching frequency. Two kinds of control interfaces utilizing analog/digital have been developed and tested. Each interface makes different system responses and, consequently, has different best gain set. Figure 7 shows the design of the faster coil current regulation loop with  $\sim 550$  us of time delays. A pair of optic isolators was installed to the interfaces between the PCS output and the IVC PS for avoiding any high-

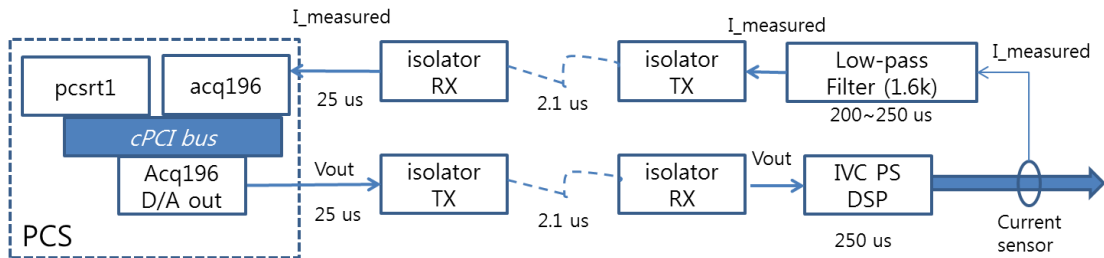


**Fig. 7. Design of the feedback loop of the KSTAR PCS for the IVC PS**

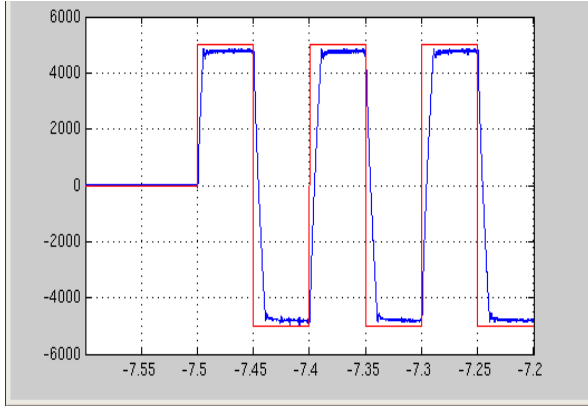


**Fig. 8. Fast swing test of the in-vessel vertical coil (IVC) with +5 kA/turn, 10 Hz.**

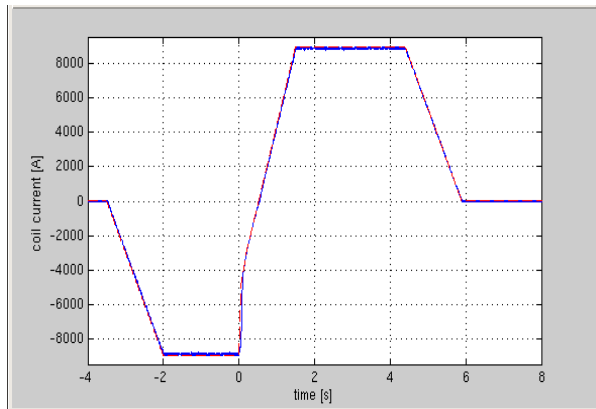


**Fig. 9. Bipolar swing example of the KSTAR PF3U from -9 kA to +9 kA/turn.**

frequency noises or ground loops. The faster loop was able to achieve coil current swings to  $\pm 5$  kA/turn with 6 turns/22.71 mH in-vessel coils as shown in Fig. 8. The algorithms for controlling bipolar operations of each PF coil have been improved to enable multiple zero-crossings with the “dead-time” within 5 ms, as shown in Fig. 9.

### 3.2. Implementations of the real-time shaping algorithms

Due to the time history dependences of the ferrite field the credibility of the EFIT reconstructions to the other diagnostics has been checked out before implementing any real-time shaping. Fig. 10 shows the reconstructed bulk properties of the EFIT for shot 2074. The results for  $R_p$ ,  $I_p$ ,  $Z_p$  and minor radius ( $A$ ) are compared with 1) estimates from the fast CCD TV ( $R_p$ ,  $Z_p$ ,  $A$ ) 2) the RC03 measurement ( $I_p$ ) and 3) a fixed boundary plasma reconstruction with all magnetic probes called as IDK [10]. The EFIT reconstruction itself was made by using 3 flux loops and 39 magnetic probes. The result showed decent match for all the methods if the measurements of the magnetic

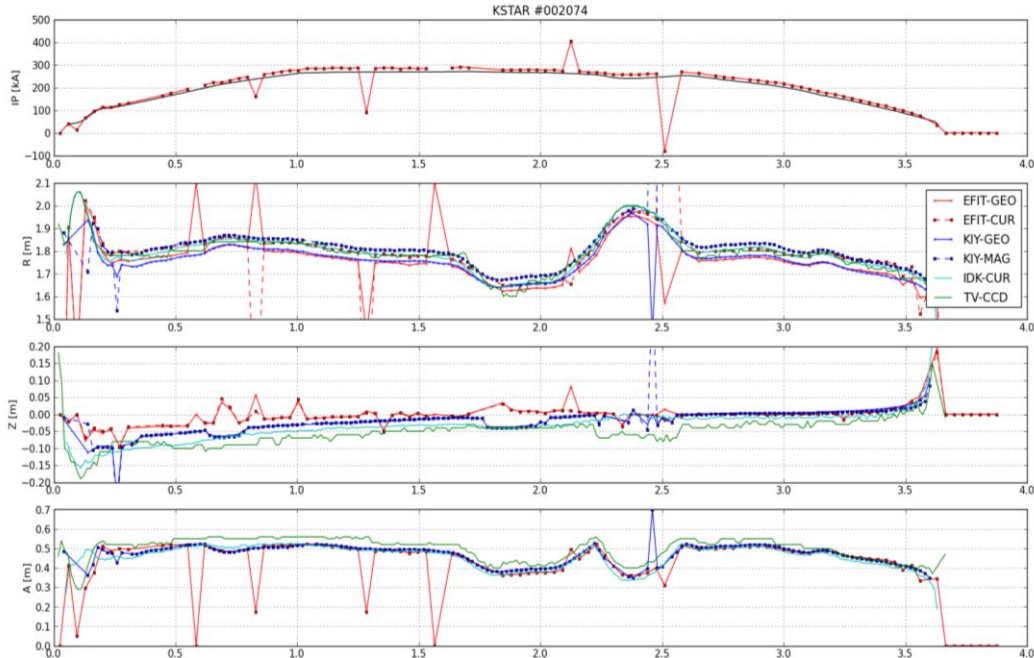


**Fig. 10. EFIT calculation (EFIT-GEO) comparison for shot 2074 with other offline estimates.**

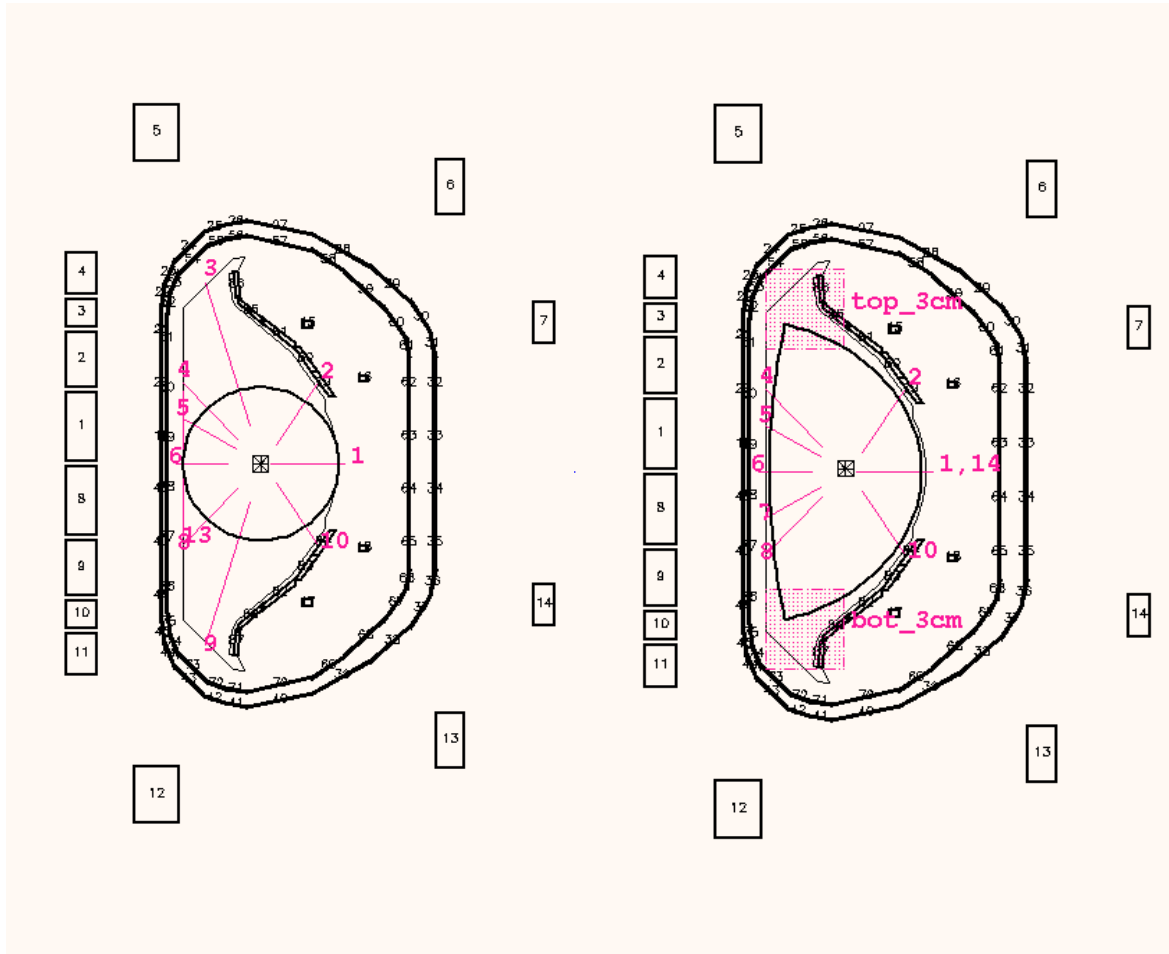


**Fig. 11. Generalized shape editor installed to the KSTAR PCS : definitions of control segments for limited/elongated plasma (left) and up/down symmetric double-null plasma (right).**

probes are close to ideal. The best match occurred from the reconstructions with the Sabbagh/Park 12-element vessel model [11].

Hence, assuming the influences of the incolloys are not very big at the Ip flattop, the implementations of the real-time shape control algorithm without incoloy908 effects have been accomplished by collaborative efforts with the DIII-D team. The basic structure of the algorithm consists of two well-known algorithms, real-time EFIT [12] and isoflux [13], with lots of customizations: The 12-element vessel model has been installed, and any real-time EFIT residing in the PCS considers the PF coil current as “unknown”, to treat them as one of the unknowns. The final answer of the fast loop EFIT, which is fed to the isoflux algorithms, consists of the outermost plasma boundary only, and the isoflux does the feedback on the “control segments” based on that information only. The control segments are defined as a straight line between the main actuator PF coil and the center of the plasma as shown in Fig. 11. The shape editor has been fully generalized to any shape which can be constructed by EFIT snapshot file. Special calibration shots for the validations of the magnetic diagnostics have been accomplished which measure individual Green function response of the diagnostic sensors by a single movement of each coil, provided all the PF coils were charged to the initial magnetization level which makes the incoloy908 in the PF CICC jackets almost saturated for 50 seconds.

### 3.3. Approaches to the diverted plasmas

The main idea of the proposed control scheme is based on the fact that the ferrite field can be regarded as a perturbation of first order. In the standard isoflux[11] shape control algorithm, the poloidal field at the target X-point should vanish. The magnetic field error at the X-point can be written as  $E_x = A1*X_p + A2*I_c + A3*I_{vv} + A4*B_m$ , where  $X_p$  includes magnetic field contributions from the plasma current elements,  $I_c$  from the superconducting/in-vessel coil currents,  $I_{vv}$  from the vessel and passive structures, and unknown contributions  $B_m$  from the nonlinear magnetic effects due to the incoloy908 material. However, the  $E_x$  still can be measurable with the pickup coils inside the vessel. The experimentally determined  $B_m$  can be utilized in the above equation and  $E_x$  treated as a feedback parameter and determine coil currents required for it to vanish at the X-point.

The initial approach for the creation of shaped plasmas will use methods to produce elongated/diverted plasmas with minimum closed loop regulations. With a reasonable offline equilibrium set, it is possible to construct sets of RZIP estimators/multipliers with considerations of decoupling each feedback loop. Then feedback can be extended on a set of single parameters such as  $I_p$ , positions of plasma center ( $Z$  and  $R$ ) and elongation ( $\kappa$ ). After an adjustable D-shape is achieved, the PCS will be able to switch the main algorithm to either RZIP/ $\kappa$ /X-point control or isoflux boundary control with real time EFIT7. The final plasma pulse scenario is expected to contain 1) a feedforward breakdown scenario, which the field null configurations are provided by offline finite element method (FEM) calculations [2], 2)  $I_p$  ramp-up and development of  $J(r)$  with outside wall growth at nearly constant  $q$  till 200~250 kA + vertical position control starting from  $t \sim 50$  ms, 3)  $I_p$  ramp up plus  $\kappa$  feedback until  $I_p = 500$  kA and 4)  $I_p$  sustain + isoflux with X-point feedback. Each step in the approach is expected to be validated by separate simulations based on the plasma data from the 2009 campaign. According to the previous plasma experiments, it is expected that reliable and accurate execution of this plasma control scenario will require sensitive regulation of the poloidal coil power supplies with multiple zero-crossing techniques, which are to be applied in the 2010 campaign. This scenario will be illustrated with experimental control results from the 2010 campaign.

- [1] G.S. Lee et al., Nucl. Fusion, 40, 575-582 (2000).
- [2] J. A. Leuer et al., IEEE transactions on plasma science, 38, 333-340 (2010).
- [3] S.W. Yoon et al., "Effect of Magnetic Materials on in-vessel magnetic configurations in KSTAR", this conference.
- [4] Y. K. Oh et al., Fus. Eng. Des., 84, 344-350 (2009).
- [5] J. Kim et al., this conference.
- [6] S. G. Lee et al., Rev. Sci. Inst. 77, 10E306 (2006).
- [7] S. H. Hahn et al., Fus. Eng. Des., 84, 867-874 (2009).
- [8] Hogun Jhang et al., Fus. Eng. Des., 65, 629 – 641 (2003).
- [9] Y. M. Jeon, "Design of optimal position and shape controller based on perturbed equilibrium response model for tokamak plasma", Ph. D Thesis, Seoul National University, Korea, 2006.
- [10] Y. M. Jeon et al., this conference.
- [11] Y. S. Park, S. A. Sabbagh et al., this conference.
- [12] J. Ferron et al., Nucl. Fusion, 38, 1055 (1998)
- [13] F. Hofmann and S. C. Jardin, Nucl. Fusion, 30, 2013 (1990).